Received: 24 September 2018 | Revised: 26 March 2019 | Accepted: 28 March 2019

DOI: 10.1002/jbio.201800368

JOURNAL OF BIOPHOTONICS

FULL ARTICLE

High-resolution imaging of fluorescent whole mouse brains using stabilised organic media (sDISCO)

Christian Hahn[1,2,3*] | **Klaus Becker**[1,2] | **Saiedeh Saghafi**[1,2] | **Marko Pende**[1,2] | **Alma Avdibašić**[2] | **Massih Foroughipour**[1,2] | **Daniel E. Heinz**[4] | **Carsten T. Wotjak**[4] | **Hans-Ulrich Dodt**[1,2*]

[1]Department of Bioelectronics, FKE, Vienna University of Technology, Vienna, Austria

[2]Center for Brain Research, Medical University of Vienna, Vienna, Austria

[3]Institute for Neuropathology, University Medical Center Göttingen, Göttingen, Germany

[4]Department of Neuronal Plasticity, Max Planck Institute of Psychiatry, Munich, Germany

***Correspondence**
Christian Hahn, Institute for Neuropathology, University Medical Center Göttingen, Robert-Koch-Straße 40, 37075 Göttingen, Germany.
Email: christian.hahn@meduniwien.ac.at
Hans-Ulrich Dodt, Department of Bioelectronics, FKE, Vienna University of Technology, Gusshausstraße 25, 1040 Vienna, Austria.
Email: dodt@tuwien.ac.at

Present address
Christian Hahn, Institute for Neuropathology, University Medical Center Göttingen, Robert-Koch-Straße 40, 37075 Gättingen, Germany.

Funding information
FWF, Grant/Award Number: P23102-N22

Optical tissue clearing using dibenzyl ether (DBE) or BABB (1 part benzyl alcohol and 2 parts benzyl benzoate) is easy in application and allows deep-tissue imaging of a wide range of specimens. However, in both substances, optical clearing and storage times of enhanced green fluorescent protein (EGFP)-expressing specimens are limited due to the continuous formation of peroxides and aldehydes, which severely quench fluorescence. Stabilisation of purified DBE or BABB by addition of the antioxidant propyl gallate efficiently preserves fluorescence signals in EGFP-expressing samples for more than a year. This enables longer clearing times and improved tissue transparency with higher fluorescence signal intensity. The here introduced clearing protocol termed stabilised DISCO allows to image spines in a whole mouse brain and to detect faint changes in the activity-dependent expression pattern of tdTomato.

KEYWORDS
EGFP, fluorescence stabilisation, light-sheet microscopy, mouse brain, optical tissue clearing, ultramicroscopy, whole-tissue imaging

1 | INTRODUCTION

Deep-tissue imaging of specimens ranging in size up to a whole adult mouse [1, 2] relies on their transparency, that is, on an obstacle-free tissue with homogenised refractive index (RI) to prevent scattering (reviewed by References [3, 4]). For RI matching, two types of optical clearing solutions can be used: aqueous or lipophilic organic media. For aqueous media, lipid barriers as cell membranes have to be rendered passable or have to be removed [5–9]. For lipophilic media, the water inside the tissue has to be exchanged by an amphipathic intermediate in the first instance (ie, dehydration).

Unfortunately, most agents used for dehydration, as methanol or ethanol, severely quench the fluorescence of enhanced green fluorescent protein (EGFP). Previously, we suggested to substitute these dehydrants by tetrahydrofuran (THF) and the clearing medium BABB (1 part benzyl alcohol and 2 parts benzyl benzoate) by dibenzyl ether (DBE) [10]. As part of clearing protocols as 3-dimensional imaging of solvent-cleared organs (3DISCO) [11] and iDISCO [12], these substances proved their versatility for different tissues and subject areas. However, degradation products of DBE and BABB such as peroxides or aldehydes detrimentally interfere with EGFP fluorescence via chemical modifications of the fluorophore [13]. Removal of these compounds before application improves EGFP fluorescence intensity and stability [10], but their regeneration is induced by even trace amounts of oxygen, water or by illumination [14] (Figure S1). To conserve EGFP signals within cleared specimens, we recently suggested a resin-based embedding for cleared samples [15]. Embedding allows both, long-term storage, as well as high illumination intensities, but no longer clearing times, limiting this method to small specimens as mouse hippocampi.

To prevent photobleaching, antifading agents are part of lab routine for fluorescence microscopy. Here, we report that propyl gallate [16–18] efficiently suppresses the re-accumulation of peroxides and aldehydes and protects EGFP fluorescence in specimens immersed in DBE or BABB. Thereby, we could overcome the drawback of these agents having an extremely high clearing potential [4, 19]. Following the terminology started with 3DISCO [11], we term this method stabilised DISCO (sDISCO).

2 | METHODS

2.1 | Animals

Thy1 EGFP-M and Thy1-YFP-H (C57BL/6) mice [20] were bred and kept at the animal care centre of the Medical University Vienna. Animal care and euthanasia were done in accordance with the ethics guidelines of the Austrian animal protection law. Experiments visualising *Arc* activation were carried out on adult male Arc-CreERT2 mice [21] (JAX stock #021881) crossed with Ai9 indicator animals (JAX stock #007909). In these animals, expression of tdTomato from the Rosa26 locus is controlled in a Cre-dependent manner given the presence of tamoxifen ($n = 6$; Max Planck Institute of Biochemistry, Martinsried, Germany). Mice were transferred to the animal facility of the Max Planck Institute of Psychiatry at age of 8 to 14 weeks, where they were housed in an inverse light-dark cycle (12 hours: 12 hours, lights off: 7 AM) under standard housing conditions (23°C ± 4°C, 50% humidity ±10%, water and food ad libitum) in type 2 macrolon cages. Experiments took place during the active phase of the circadian rhythm (between 9 AM and 6 PM). All experimental procedures were carried out according to the European Community Council Directive 2010/63/EEC and were approved by the Government of Upper Bavaria.

2.2 | Preparation of mouse brains

Before transcardial perfusion, the mice were sacrificed using carbon dioxide or Isoflurane (CP-Pharma GmbH, Germany). After washing out the blood with 50 mL ice-cold PBS (Biochrome, Germany) adjusted to pH 8.3 including 10 units/mL Heparin (Heparin-Natrium-25 000, Ratiopharm, Germany), fixation was performed using 100 mL ice-cold 4% paraformaldehyde (Roth, Germany)/PBS adjusted to pH 8.3. Brains were dissected and fixation was continued at 4°C for overnight.

2.3 | Purification of THF, DBE and BABB

The purification of clearing chemicals from peroxides and aldehydes is described in detail [10]. In brief, the liquids were purified by column chromatography using aluminium oxide (activated basic, Brockmann I [very dry], Sigma-Aldrich, Germany). Then, the absence of peroxide and aldehyde contents was verified using Quantofix-25 strips (Macherey-Nagel, Germany) and by Brady's test [22]. Possible remaining or accumulated trace amounts of water within the liquids were removed by addition of molecular sieve beadlets with 0.3 nm diameter pore size (Sigma-Aldrich, Germany). To prevent re-accumulation of peroxides and aldehydes, 250 mg/L butylated hydroxytoluene (SAFC, Sigma-Aldrich, Germany) was added to THF and 0.4% propyl gallate was added to DBE and BABB. Propyl gallate dissolves in DBE or BABB after a few minutes stirring at room temperature. Important safety caution: During THF purification, the necessary stabiliser provided by the company is removed. Butylated hydroxytoluole must be added directly after purification, since insufficient stabilised THF can explode after prolonged exposure to oxygen and/or sunlight. Also Brady's reagent must be handled with care, since 2-4-dinitrophyenylhydrazine is explosive and methanol is toxic.

2.4 | Optical tissue clearing of brains

After postfixation, brains were washed three times with PBS pH 8.3. If required, they were split into hemispheres. Then, the specimens were dehydrated with THF (Roth, Germany) and optically cleared in DBE (Merck Millipore, Germany) [10] or in BABB (benzyl alcohol from Sigma-Aldrich, Germany, benzyl benzoate from Merck Millipore, Germany).

Brains were dehydrated in a series of ascending concentrations of THF, that is, 30%, 50%, 70% (in PBS pH 8.3), 80%, 90% and 96% (in water) and finally pure THF. Two to three dehydration steps were performed per day. Then, the brains were incubated at least three times for 12 hours and 1 day in THF in the presence of molecular sieve beadlets. Substitution of THF by DBE or BABB was done successively, that is, briefly in 50%, 70%, 80%, 96% and then pure (three times) until the specimens became clear. Propyl gallate (Sigma-Aldrich, Germany) was dissolved in DBE or BABB in a concentration of 0.4%. During all incubations steps and during storage, the specimens were kept at 4°C, and during clearing on a horizontal shaker. For statistical analysis of signal protection, brains of three Thy1-EGFP-M mice were divided in hemispheres. From each brain, one hemisphere was optically cleared using 3DISCO [10], the corresponding other hemisphere was optically cleared using sDISCO. Fluorescence was imaged directly after clearing and 1 month later. The fluorescence was measured using ImageJ and signal to noise ratio was calculated.

2.5 | Activity controlled expression of tdTomato and preparation of the mouse brains

To trigger expression of tdTomato in an activity-dependent manner, mice were assigned to two groups (each $n = 3$) and treated with 100 mg/kg tamoxifen i.p. (Sigma-Aldrich, Germany). Twelve hours later, the experimental group was exposed to an elevated plus maze (EPM) without side and end walls for 30 minutes, whereas the control group stayed in the home cage. The test was performed under low light conditions (<40 lux). Exposure to the novel, arousing environment was chosen to maximise *Arc* expression [21]. Sixteen days later, the mice were sacrificed by an overdose of Isoflurane.

2.6 | Ultramicroscopy and image processing

Specimens were fixed and positioned with a vascular clamp (S&T, Switzerland) mounted on a custom-made 30-deg ramp, both made of stainless steel. Imaging was performed using a modified version of the ultramicroscopy setup as described [23]. This modified system is equipped with two Sapphire lasers (Coherent Inc., Germany) emitting a 488 and 532 nm continuous Gaussian beam for fluorescence excitation and a custom-made light sheet generator [24]). The data for Figure S4 were measured using a standard ultramicroscopy setup as described [25]. Recording was done using an Andor Neo CMOS camera (Andor, Ireland) with 2560 x 2160 pixel resolution. Microscopy was done using Olympus objectives (XLFLUOR 2x NA = 0.14, XLFLUOR 4x NA = 0.28, and LUCPLFLN 20x NA = 0.45), corrected to the RI of ~1.56 by custom-made modulator units [24] or a 25x objective (XLSLPlan N, NA = 1.0, Olympus, Tokyo, Japan) with integrated RI adjustment. We used a 525/50 nm filter for EGFP, a 550/49 nm filter for YFP and a 605/70 nm filter for tdTomato.

After recording, the images were computationally post-processed by deconvolution, contrast-limited adaptive histogram equalisation (CLAHE) and destriping using custom-made software. Three-dimensional (3D)-reconstruction was done by using AMIRA 6.1 (Thermo Fisher, Germany).

2.7 | Imaging with confocal and STED microscopy

Brains from adult Thy1-YFP-H mice were perfused, post-fixed and washed as described. Thereafter, the brains were cut into 600 μm thick coronal slices using a vibratome and then optically cleared as described. To prevent bending of the slices during dehydration, they were flattened under a coverslip burdened by a small block of stainless steel. After clearing using stabilised DBE, the slices were mounted within stabilised DBE in between a slide and a coverslip adhered by a ring of two-component epoxy-based adhesive (UHU plus schnellfest, UHU GmbH & Co KG, Germany). The images were recorded with a Leica SP8-gSTED super-resolution microscope using different settings for confocal and STED imaging (BOKU VIBT Imaging Centre in Vienna, Austria).

2.8 | uDISCO and FluoClearBABB

Optical tissue clearing was performed as described [2, 26] to compare sDISCO with uDISCO and FluoClearBABB. For each comparison, three YFP-H mouse brains were divided into hemispheres. One hemisphere of each brain was optically cleared according to the sDISCO protocol and the corresponding hemisphere according to the uDISCO or the FluoClearBABB protocol. For uDISCO, the hemispheres were dehydrated in ascending concentrations of *tert*-butanol (Sigma-Aldrich, Germany) in distilled water of 30% (overnight), 50% (4 hours), 70% (4 hours), 80% (overnight), 90% (4 hours), 96% (4 hours) and finally in pure *tert*-butanol (overnight). Then, the hemispheres were incubated in dichloromethane (Sigma-Aldrich, Germany) for 45 minutes and finally cleared in BABB-D4 (BABB 4:1 with diphenyl ether (Roth, Germany)) with 0.4% alpha-tocopherol (Sigma-Aldrich, Germany). For FluoClearBABB, *tert*-butanol and BABB were adjusted to pH 9.5 with triethylamine (Sigma-Aldrich, Germany). The hemispheres were dehydrated in ascending concentrations of adjusted *tert*-butanol in distilled water of 30% (overnight), 50% (over day), 70%

(overnight), 80% (over day), 96% (overnight) and finally two times in pure *tert*-butanol (over day, overnight). Finally, the hemispheres were optically cleared in adjusted BABB. All hemispheres were recorded with light-sheet microscopy using one-side illumination and a 4-fold objective with 2-fold postmagnification. Therefore, equivalent sections were illuminated constantly for 14 minutes. Every 2 minutes, an image was recorded, and its histogram was determined using ImageJ and an integral calculated. The measurements were done directly after clearing and 1 week later.

3 | RESULTS

3.1 | Optical tissue clearing and stabilisation of fluorescence

For optical tissue clearing, the use of organic clearing agents such as DBE or BABB is as potent as economic, but the fugacity of fluorescence within these media has always been considered as the drawback of these methods. Although DBE itself is inert to fluorescent proteins as EGFP, it reacts with oxygen or light forming peroxides and aldehydes [14] that severely deteriorate fluorescent signals. Purification of DBE by column chromatography with basic activated aluminium oxide efficiently removes peroxides and aldehydes [10, 27]. However, both contaminants are regenerating within the purified medium. Since peroxides and aldehydes develop subsequently (Figure S1), the ability to prevent the generation of peroxides as the initial step in this reaction chain is essential for a stabiliser.

To find a substance that prevents peroxide generation and stabilises fluorescence in DBE, we tested several chemical compounds. Some of these substances do not dissolve in DBE, are severely toxic as, for example, p-phenyldiamine, or impair the clearing result as 1, 4-diazabicyclo [2],2,2 octane (DABCO). Among further antioxidants tested, we found propyl gallate [16, 28] to have the highest capacity to eliminate peroxides from DBE. After addition of propyl gallate, peroxides (10 mg/L) are eliminated within 1 minutes, while we could not find elimination of peroxides with butylhydroxyltoluol, butylhydroxylanisol or alpha-tocopherol in a comparable time. Next, we tested the ability of propyl gallate to suppress the accumulation of peroxides and aldehydes in purified DBE. To accelerate their formation, we let air bubbling through DBE inside a cold trap. Without stabiliser, critical peroxide levels accumulated quickly. Using Brady's test for aldehydes [22], we found accumulating aldehydes with a short delay. After 1 day, we detected 0.5 mg/L peroxides and after 3 days, 2 mg/L peroxides as well as aldehydes. We repeated the experiment in the presence of 0.2% (w/v) propyl gallate. We could not detect any peroxides or aldehydes even after 1 month under air bubbling or after 1 year in a specimen's container stored at 4°C.

Dissolving of propyl gallate gives DBE a slightly yellowish tint. At 488 nm, transmission is reduced by less than 1% in a solution of 1% propyl gallate in DBE compared to pure DBE (91.9% down to 91.1%) measured in a quartz cuvette with a spectrophotometer (Hitachi-5100, Hitachi, Japan). For concentrations used for microscopy, the interference with light is much lower and thus negligible.

To test whether propyl gallate interferes with the transparency of the specimens, we placed a mouse brain that was optically cleared in DBE stabilised with 0.4% propyl gallate on an USAF 1951 chart (Figure 1A). On an image taken with 8-fold magnification the 7-6 lines are distinguishable, confirming a resolution of at least 2.19 µm through the whole brain (Figure 1B). We therefore conclude that propyl gallate in this concentration is compatible with high-resolution imaging.

To test the effect of propyl gallate on fluorescent proteins within biological specimen, we optically cleared brains and thick brain slices of Thy1-EGFP-M and Thy1-YFP-H mice and imaged the specimens with different techniques. Using confocal microscopy, we could achieve high structural resolution in optically cleared 600 µm thick slices of Thy1-YFP-H mice (Figure 1C) during repetitive illumination.

To address whether the fluorescence protection by propyl gallate is sufficient for STED microscopy [29], we subsequently imaged the same specimen using a STED setup (Leica). Common settings were chosen and the hippocampal formation was imaged. Thereby neurites could be imaged with high resolution revealing spines (Figure 1C, inset).

To quantify the signal protective effect of propyl gallate over time, we split three perfusion-fixed EGFP expressing mouse brains into hemispheres and cleared one hemisphere in DBE containing propyl gallate (stabilised DBE) and the complementary hemisphere in DBE without propyl gallate as a control. After achieving transparency, an equivalent optical plane in all hemispheres was selectively illuminated and measured using ultramicroscopy. After 1 month, we imaged the same hemispheres again. While the signal was almost gone within the nonstabilised hemispheres (3DISCO) (Figure 1D), it was still bright within the hemisphere in stabilised DBE (sDISCO) (Figure 1E). Without stabilisation, the signal to noise ratio (SNR) dropped to 0.24 ± 0.05, whereas it kept stable at 1.04 ± 0.15 with stabilisation (Figure 1F; $P < 0.01$, Student's t test). Since the optical clearing process keeps ongoing, transparency and clearing quality can be significantly improved with longer clearing

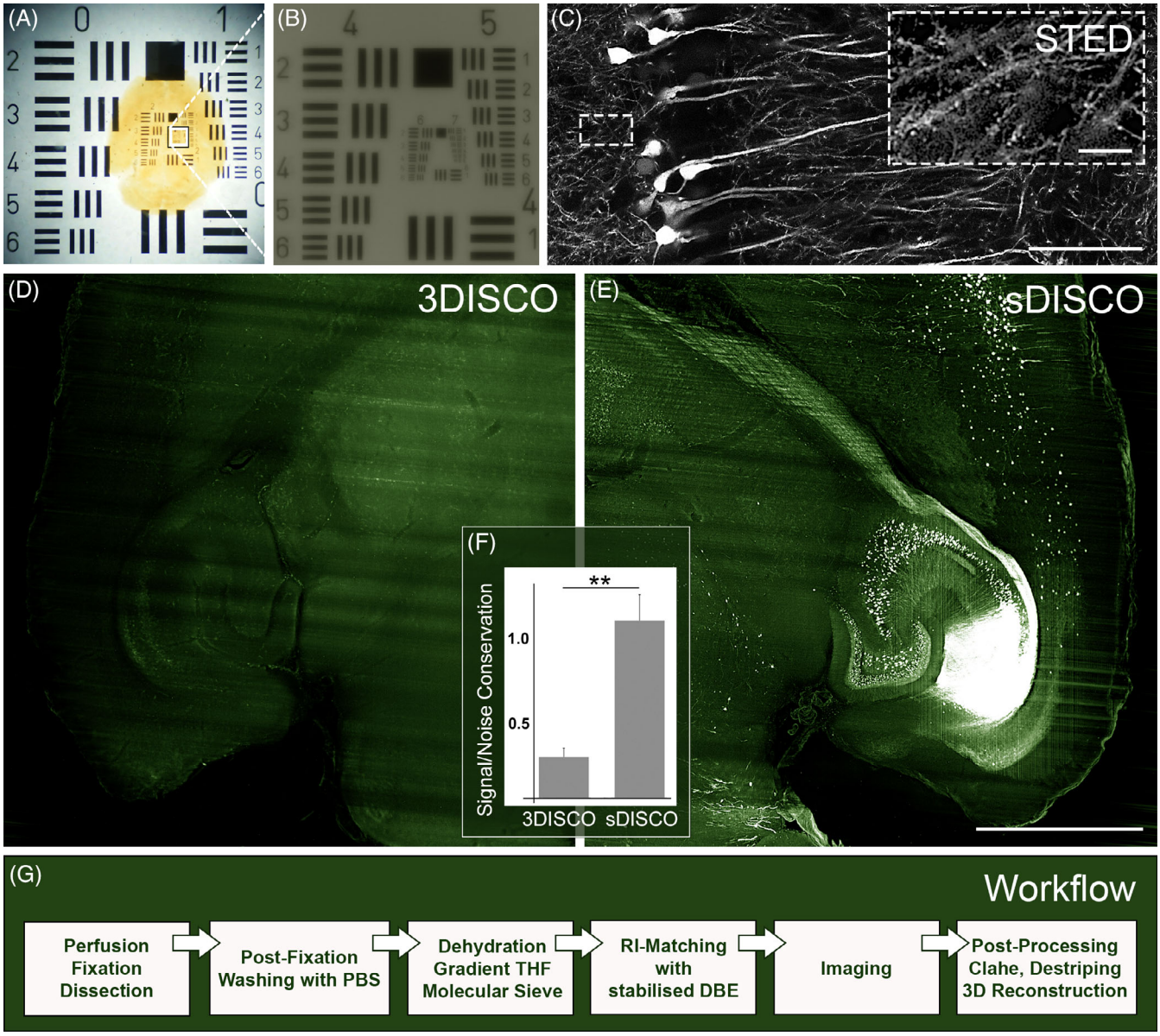

FIGURE 1 Optical clearing and stabilisation of fluorescence. (A, B) A mouse brain cleared with stabilised DBE placed on top of a USAF 1951 chart demonstrates a resolution through the whole brain down to about 2 µm. (C) The overview image shows a part of the hippocampal formation in an optically cleared thick slice of a Thy1-YFP-H mouse brain recorded by confocal microscopy using a 40-fold objective (Leica). In pyramidal cells, YFP fluorescence was detected within dendrites up to the tips of their arborisation. Subsequent recording of a small area (small inset) by STED microscopy using a 100-fold objective (Leica) reveals spines with high resolution (large inset). The scale bars represent 50 µm in the overview image and 5 µm in the inset. (D, E) Comparison of signal preservation in purified but nonstabilised DBE (3DISCO) and in stabilised DBE (sDISCO) in hemispheres of the same Thy1-GFP-M mouse brain. (D) After 1 month, EGFP fluorescence is almost vanished in the hemisphere immersed in nonstabilised DBE. (E) Within stabilised DBE, the fluorescence signal remained. The hemispheres were illuminated from one side using an aspheric ultramicroscope and imaged using a corrected 4-fold objective (Olympus, (XLFLUOR 4x NA = 0.28). The scale bar represents 1 mm. (F) In 3DISCO, the signal to noise ratio after clearing drops to 24% after 1 month, in sDISCO, it remains almost constant during this time interval ($n = 3$, Student's t test, two-tailed, $P < 0.01$). Error bars represent standard deviations. (G) Scheme of the whole sDISCO workflow

times, opening windows for clearing of larger specimens or tissues that are more difficult to clear. Even after almost 2 years (22 months) storage time, EGFP fluorescent brains optically cleared in stabilised DBE could be recorded with structural details (Figure S2).

Purification of DBE by chromatography using basically activated water-free (Brockmann I) aluminium oxide removes, besides water and peroxides, also contaminations with aldehydes [27]. To find out, to what extent peroxides contribute to bleaching of EGFP, we examined

whether the elimination of peroxides would be sufficient to preserve fluorescence. Therefore, we removed peroxides within not purified DBE by adding propyl gallate (stabilised not purified DBE). According to the Quantofix-25 peroxide test strips, peroxides disappeared almost immediately after addition. Then, we divided mouse brains into hemispheres and compared fluorescence conservation within not purified DBE with not purified stabilised DBE. We further compared fluorescence conservation in not purified DBE with purified stabilised DBE. The fluorescence preservation in stabilised not purified DBE was similarly poor as in not purified DBE and much worse compared to DBE that was purified and stabilised directly after purification (Figure S3). Thus, peroxides themselves are not the only factor quenching fluorescence. However, blocking of peroxides in previously purified DBE preserves EGFP fluorescence for a very long time. Since aldehydes are known to severely quench the fluorescence of EGFP and since aldehydes are only formed in the presence of peroxides [14], we conclude that neutralising peroxides prevents fluorescence bleaching by blocking the emergence of aldehydes.

To improve EGFP fluorescence, we increased the pH [26, 30] to 8.3 in our clearing protocol during fixation and washing and kept the storage temperature at 4°C. Figure 1G describes the whole workflow of the sDISCO clearing procedure.

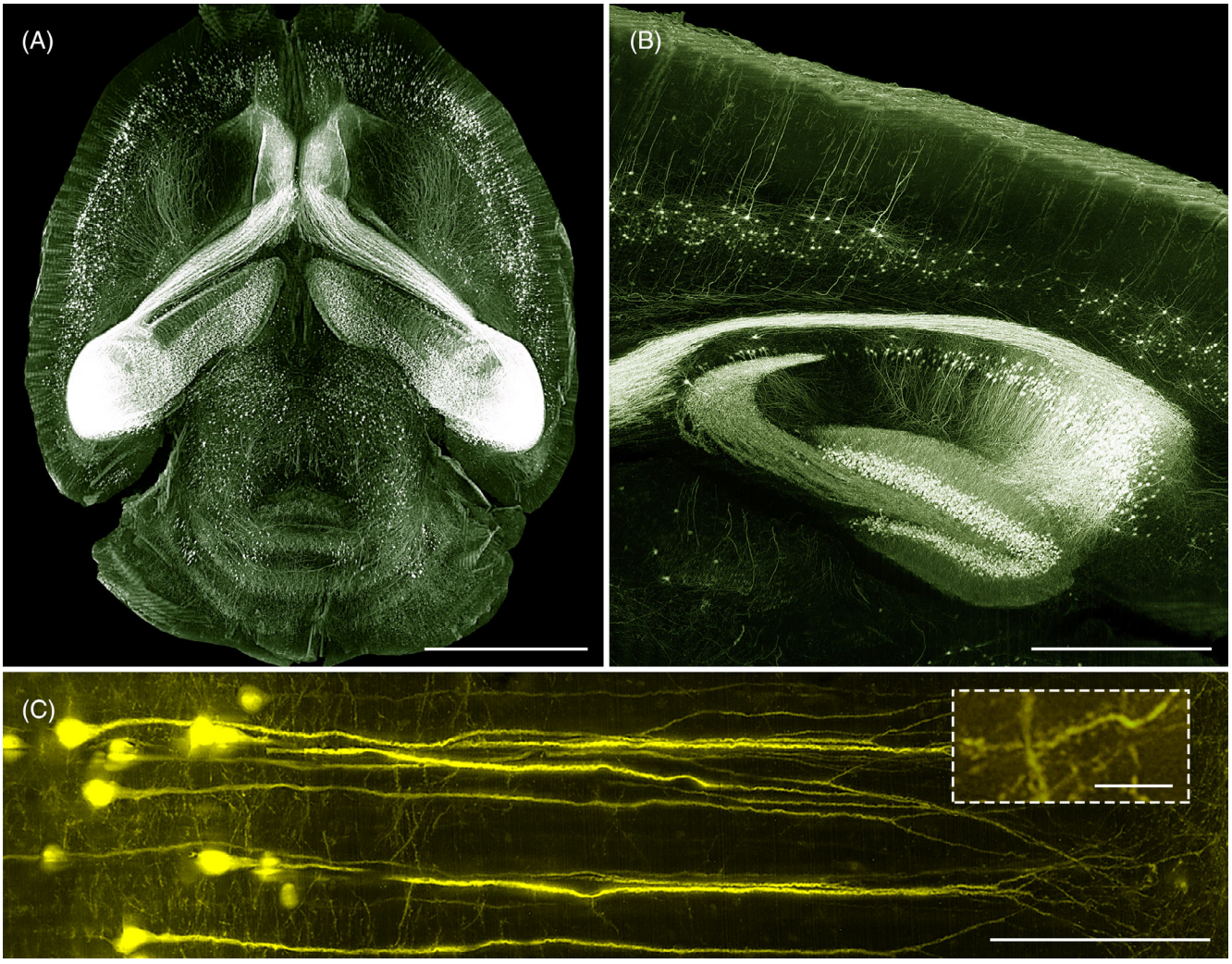

FIGURE 2 Imaging of whole mouse brains optically cleared with stabilised DBE. (A) For imaging a Thy1-EGFP-M brain in its entirety, it was illuminated using aspheric light-sheet generators from two sides. Images were taken using a corrected 4-fold objective combined with a 0.5-fold postmagnification. The surface of the brain was computationally removed using a digital erosion filter (MATLAB). A virtual section comprising the whole hippocampal formation was reconstructed. The scale bar represents 2 mm. (B) By combining the corrected 4-fold objective with a 2-fold postmagnification, subcellular structures of neurons in the cortex and the hippocampal formation as axons and dendrites can be resolved. The scale bar represents 0.5 mm. (C) Recording a Thy1-YFP-H mouse brain with a corrected 25x Olympus objective XLSLPlan N (NA = 1.0) resolves fine details including spines of cortical neurons (inset). The scale bars represent 100 µm in the overview and 20 µm in the inset

3.2 | sDISCO allows imaging of whole mouse brain as well as details with subcellular resolution

To test the effectiveness of stabilised DBE clearing, we optically cleared and recorded whole brains of Thy1-EGFP-M and Thy1-YFP-H mice using an aspheric ultramicroscope [23]. We imaged the brains with different objectives and settings. In combination of a 4-fold objective with a 2-fold postdemagnification, a whole adult mouse brain could be imaged at once (Figure 2A, Movie S1). Structures of the hippocampal formation and cortical neurons could be visualised including their fine arborisations (Figure 2B, Movie S2). Using a 25x objective, dendritic spines could be resolved within a whole brain (Figure 2D, inset).

Analogously to the stabilisation of DBE, we purified and stabilised BABB. We found, that the EGFP signal was also preserved in stabilised BABB (Figure S4).

3.3 | Imaging of neuronal activity-mediated tdTomato expression

Optical clearing of whole mouse brains has been frequently used to visualise their overall system's architecture labelled, for example, by constitutively expressed fluorophores within neuronal subpopulations [2, 25]. Due to the high expression levels of these reporters, a relative low signal-to-noise ratio (SNR) is sufficient for measurements. In comparison, the expression levels due to neuronal activity, for example, of immediate early genes (IEG), are more subtle. The good SNR of the images obtained from Thy1-EGFP-M mouse brains cleared with sDISCO encouraged us to ask, whether sDISCO enables elucidation of activity traces. We measured activity patterns upon behavioural stimulation. To generate these activity patterns, Arc-CreERT2 mice [21] were crossed with the Ai9 indicator line. Adult offspring were treated with tamoxifen 12 hours before exposure to an aversive environment; control mice remained undisturbed in their home cages. We collected the brains 16 days later. Activation of the *Arc* promotor due to increased neuronal activity triggers the synthesis of the Cre-recombinase, which translocates into the nucleus only in presence of tamoxifen. Within the nucleus, Cre cleaves a stop-codon from the tdTomato gene. Consequently, behaviour-driven neuronal activity can be visualised by changes in the expression of tdTomato. We measured the tdTomato expression using a 532 nm laser and autofluorescence using a 488 nm laser as structural reference after optical clearing within stabilised DBE. After registration of the tdTomato expression pattern to the autofluorescent brain structure, we could detect group differences in *Arc*-dependent tdTomato expression within specific neuronal populations such as the hippocampal formation (both CA1 and dentate gyrus) and in axons of corticothalamic projections as described [21] (Figure 3, Movie S3).

3.4 | Comparison with established techniques for optical tissue clearing

To see how sDISCO performs in signal stabilisation in comparison with established techniques applying organic media for refractive-index matching, we compared sDISCO with uDISCO and FluoClearBABB and measured signal conservation during constant illumination. We divided YFP-expressing brains into hemispheres and cleared each one hemisphere according to the sDISCO and the corresponding with uDISCO ($n = 3$) and FluoClearBABB ($n = 3$). We recorded each hemisphere with light-sheet microscopy using one-side illumination and a 4-fold objective with 2-fold postmagnification. Equivalent sections were illuminated constantly for 14 minutes to evaluate the effectiveness of propyl gallate as a fluorescence stabiliser during illumination. Any 2 minutes, an image was recorded, its histogram determined and its integral calculated. The experiment was repeated after 1 week. After 14 minutes, the sDISCO signal is reduced to 65.6 ± 5.2% (mean ± SEM) during the first measurement and to 51.2 ± 6.0% during the second measurement. In contrast, FluoClearBABB drops to 47.3 ± 3.8% during the first measurement and to 20.3 ± 8.5% during the second measurement. The uDISCO signal drops to 59.7 ± 3.1% during the first measurement and to 44.4% ± 3.1% during the second measurement (Figure S5). Thus, in stabilised media, the fluorescence is better preserved during illumination than in FluoClearBABB.

4 | DISCUSSION

Propyl gallate is a synthetic nontoxic derivative of gallic acid and widely used as antioxidant in food and cosmetics industry. It was described as an extremely potent scavenger towards hydroxyl radicals, much stronger than, for example, alpha-tocopherol [31] and its antioxidant activity was calculated above reference compounds in a lipid medium [18]. We found, that addition of propyl gallate to organic clearing solvents as DBE or BABB protects fluorescence of YFP, tdTomato, and of EGFP for more than 1 year. We added 0.4% propyl gallate directly after purification of DBE by column chromatography with activated aluminium oxide to block the reformation of peroxides.

To obtain optimal fluorescence preservation, we kept the specimens at 4°C and shifted the pH from physiologic values to 8.3, where fluorescence of EGFP and YFP is almost 100% [32]. At basic conditions, the conformation of EGFP is more closed and the fluorophore is more fluorescent [13]. We assume, that fixation at these conditions conserves this closed conformation of the fluorophore protecting the fluorophore's core from consecutive covalent

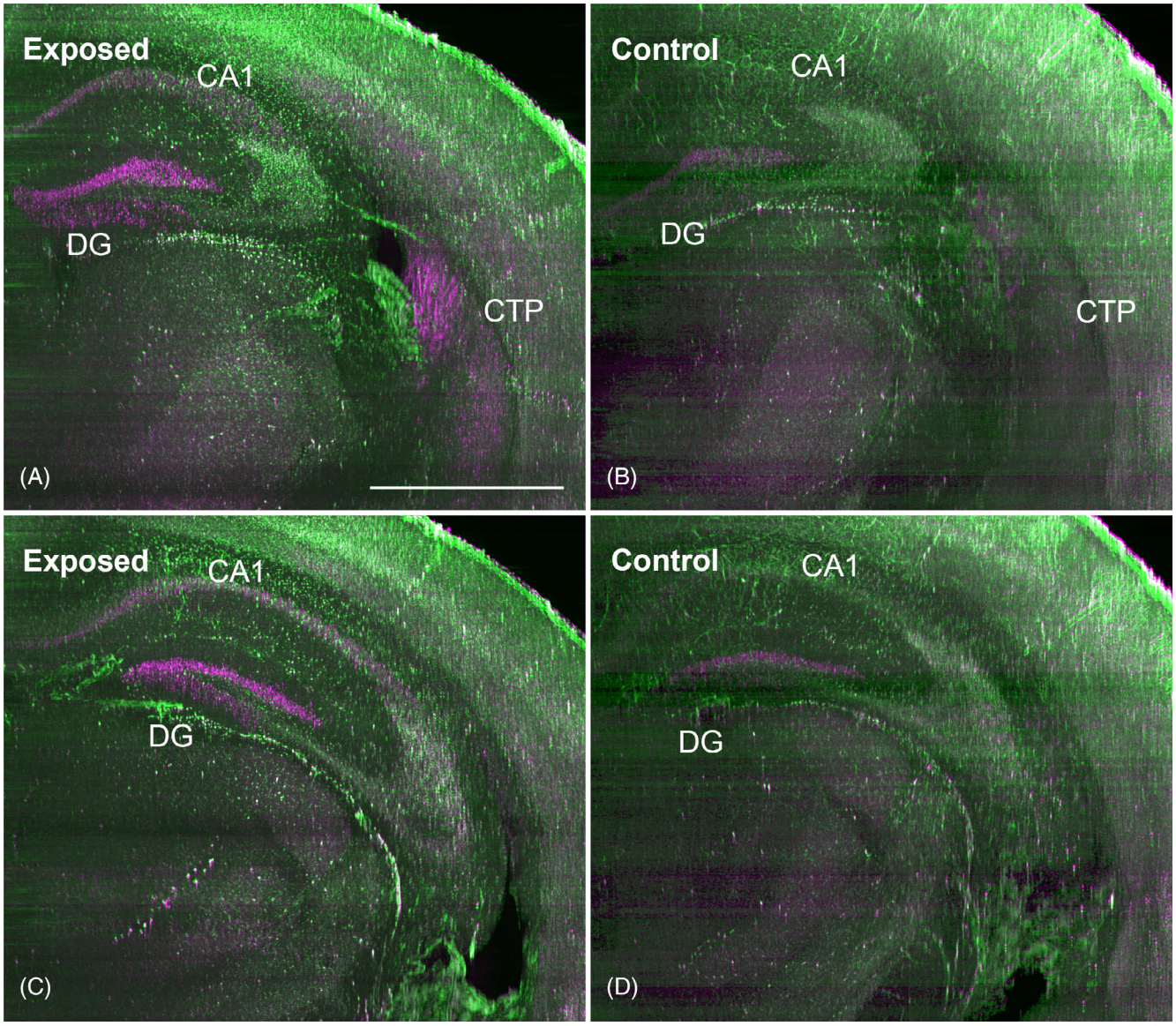

FIGURE 3 Imaging of the immediate early gene (IEG) Arc-related neuronal activity patterns. Whole brains of mice expressing tdTomato depending on activation of the arc promotor were optically cleared using stabilised DBE. The brains were recorded using one-sided illumination and a RI-corrected 4-fold objective. (A, C) TdTomato fluorescence was excited using a 532 nm laser light (pink representation). As structural reference, autofluorescence was evoked by 488 nm laser light (green representation). Images were processed using a tophat morphological filter, histogram equalisation (both MATLAB) and FFT-based destriping. (B, D) Basal expression of tdTomato under control conditions is visible in the dentate gyrus and the thalamus. (A, C, representative layers) Following exposure of the mice to an aversive environment, tdTomato expression is most dramatically upregulated in neurons of the CA1 region, the dentate gyrus (DG) and within axons of some corticothalamic projections (CTP). (B and D are corresponding layers to A, C) In these images, Arc activity is shown about −2.3 mm (A, B) respectively 2.9 mm relative to the Bregma (C, D). The scale bar represents 1 mm

modifications by reactive molecules as peroxides or aldehydes.

Remnants of blood, for example, in mouse brains lead to a labelling of blood vessels, which is probably due to a chemical reaction of propyl gallate with the iron cations of haemoglobin. A slight amber overall colourisation of the specimens, which does not interfere with imaging, is probably caused by a similar reaction. However, a careful perfusion can sufficiently avoid labelling of blood vessel and unwanted background. Advantageously, the overall background fluorescence seems to be reduced in the presence of propyl gallate. In case that blood cannot be removed adequately before optical tissue clearing, one could try to remove iron cations using chelators as, for example, EDTA at slightly basic buffered conditions.

Signal stabilisation by sDISCO enables not only analysis of the physical structures of neuronal networks including the visualisation of spines in whole mouse brains, but also the visualisation of neuronal activity patterns. In combination

with fluorescent reporters and light-sheet microscopy, the entirety of activated *Arc*-expressing neurons within a whole mouse brain can be visualised. This enables fast identification of cell populations, which are active in certain tasks.

As well as with light-sheet microscopy, sDISCO can be easily used with confocal or STED microscopy, enabling the analysis of details with very high resolution. We applied both confocal microscopy and STED at standard settings. We found that stabilised DBE protects fluorescence in specimens also during repetitive STED recordings. This allows resolving spines with more details compared to confocal microscopy.

Recently, advantages of both tissue expansion [33, 34] and shrinkage [2] for deep tissue imaging were discussed. For clearing with organic solvents, dehydration leads to compaction of approximately 30% in each dimension for mouse brains. This is similar for 3DISCO [10, 11], uDISCO [2], sDISCO and FluoClearBABB [26].

In contrast to organic liquids as DBE or BABB, highly saturated viscous solutions containing sugars as sucrose [7], fructose [35], sorbitol [36] or polyiodide compounds as Histodenz [8, 37], exhibit more turbidity with streaks and cloudiness causing light scattering [38] along the light pathways. In deep-tissue imaging, the length of the light pathways for illumination and detection sums up to several cm making even small improvements in the optical quality, that is, optic homogeneity of the medium advantageous for the imaging quality. In contrast to uDISCO, stabilised DBE consists of just two compounds and is less toxic. We found the RI of 1.561 suitable for clearing of different tissues (data not shown). However, if adaptation is desired, stabilised BABB could be mixed in varied mixing ratios.

The fluorescence signal is better preserved within stabilised optical tissue clearing media during long-term illumination. In contrast to uDISCO [39], sDISCO is compatible with tdTomato.

Beside its excellent fluorescence preservation, a major advantage of sDISCO is the simplicity of the clearing procedure with a nontoxic add-on, the easy handling and long-term storage of the specimens. Since the optical clearing process keeps going on with time, tissue transparency can be significantly improved because by using sDISCO there is no need to compromise between processing time and quality of fluorescence preservation. This opens new windows for working with larger specimens or tissues that are more difficult to clear.

ACKNOWLEDGMENTS

The study was funded by FWF, Project Number P23102-N22. We thank all lab members of the Department for Bioelectronics at the FKE, Technical University Vienna and the Section for Bioelectronics at the Center for Brain Research, Medical University Vienna and for discussion and commenting on the manuscript text.

CONFLICT OF INTEREST

The authors declare no potential conflict of interest.

AUTHOR CONTRIBUTIONS

C.H., K.B. and C.T.W. designed the study. C.H. developed the sDISCO protocol and performed most of the experiments. S.S. designed the aspheric ultramicroscope and corrected the objectives for a RI of 1.56. M.P. and A.A. contributed with experiments. D.E.H. performed the experiments with the Arc mice. C.H. and K.B. wrote the manuscript. C.H., K.B. and M.F. made the figures and movies. H.-U.D. contributed materials and methods. All authors discussed the results and commented on the manuscript text.

AUTHOR BIOGRAPHIES

Please see Supporting Information online.

ORCID

Christian Hahn https://orcid.org/0000-0003-0110-6467
Hans-Ulrich Dodt https://orcid.org/0000-0002-9784-9689

REFERENCES

[1] K. Tainaka, S. I. Kubota, T. Q. Suyama, E. A. Susaki, D. Perrin, M. Ukai-Tadenuma, H. Ukai, H. R. Ueda, *Cell* **2014**, *159*, 911.
[2] C. Pan, R. Cai, F. P. Quacquarelli, A. Ghasemigharagoz, A. Lourbopoulos, P. Matryba, N. Plesnila, M. Dichgans, F. Hellal, A. Erturk, *Nat. Methods* **2016**, *13*, 859.
[3] J. Seo, M. Choe, S. Y. Kim, *Mol. Cells* **2016**, *39*, 439.
[4] K. Tainaka, A. Kuno, S. I. Kubota, T. Murakami, H. R. Ueda, *Annu Rev Cell Dev Biol* **2016**, *32*, 713.
[5] K. Chung, J. Wallace, S. Y. Kim, S. Kalyanasundaram, A. S. Andalman, T. J. Davidson, J. J. Mirzabekov, K. A. Zalocusky, J. Mattis, A. K. Denisin, S. Pak, H. Bernstein, C. Ramakrishnan, L. Grosenick, V. Gradinaru, K. Deisseroth, *Nature* **2013**, *497*, 332.
[6] E. Murray, J. H. Cho, D. Goodwin, T. Ku, J. Swaney, S. Y. Kim, H. Choi, Y. G. Park, J. Y. Park, A. Hubbert, M. McCue, S. Vassallo, N. Bakh, M. P. Frosch, V. J. Wedeen, H. S. Seung, K. Chung, *Cell* **2015**, *163*, 1500.
[7] E. A. Susaki, K. Tainaka, D. Perrin, F. Kishino, T. Tawara, T. M. Watanabe, C. Yokoyama, H. Onoe, M. Eguchi, S. Yamaguchi, T. Abe, H. Kiyonari, Y. Shimizu, A. Miyawaki, H. Yokota, H. R. Ueda, *Cell* **2014**, *157*, 726.

[8] B. Yang, J. B. Treweek, R. P. Kulkarni, B. E. Deverman, C. K. Chen, E. Lubeck, S. Shah, L. Cai, V. Gradinaru, *Cell* **2014**, *158*, 945.
[9] M. Pende, K. Becker, M. Wanis, S. Saghafi, R. Kaur, C. Hahn, N. Pende, M. Foroughipour, T. Hummel, H. U. Dodt, *Nat. Commun.* **2018**, *9*, 4731.
[10] K. Becker, N. Jahrling, S. Saghafi, R. Weiler, H. U. Dodt, *PLoS One* **2012**, *7*, e33916.
[11] A. Erturk, K. Becker, N. Jahrling, C. P. Mauch, C. D. Hojer, J. G. Egen, F. Hellal, F. Bradke, M. Sheng, H. U. Dodt, *Nat. Protoc.* **2012**, *7*, 1983.
[12] N. Renier, Z. Wu, D. J. Simon, J. Yang, P. Ariel, M. Tessier-Lavigne, *Cell* **2014**, *159*, 896.
[13] A. A. Alnuami, B. Zeedi, S. M. Qadri, S. S. Ashraf, *Int J Biol Macromol* **2008**, *43*, 182.
[14] F. G. Eichel, D. F. Othmer, *Ind Eng Chem* **1949**, *41*, 2623.
[15] K. Becker, C. M. Hahn, S. Saghafi, N. Jahrling, M. Wanis, H. U. Dodt, *PLoS One* **2014**, *9*, e114149.
[16] H. Giloh, J. W. Sedat, *Science* **1982**, *217*, 1252.
[17] K. D. Krenik, G. M. Kephart, K. P. Offord, S. L. Dunnette, G. J. Gleich, *J. Immunol. Methods* **1989**, *117*, 91.
[18] M. E. Medina, C. Iuga, J. R. Alvarez-Idaboy, *Phys. Chem. Chem. Phys.* **2013**, *15*, 13137.
[19] P. Wan, J. Zhu, J. Xu, Y. Li, T. Yu, D. Zhu, *Neurophotonics* **2018**, *5*, 035007.
[20] G. Feng, R. H. Mellor, M. Bernstein, C. Keller-Peck, Q. T. Nguyen, M. Wallace, J. M. Nerbonne, J. W. Lichtman, J. R. Sanes, *Neuron* **2000**, *28*, 41.
[21] C. J. Guenthner, K. Miyamichi, H. H. Yang, H. C. Heller, L. Luo, *Neuron* **2013**, *78*, 773.
[22] O. L. Brady, G. V. Elsmie, *Analyst* **1926**, *51*, 77.
[23] S. Saghafi, K. Becker, C. Hahn, H. U. Dodt, *J. Biophotonics* **2014**, *7*, 117.
[24] S. Saghafi, K. Becker, C. Hahn, M. Pende, N. Jahrling, M. Wanis, I. Sabdyusheva-Litschauer, M. Foroughipour, A. Niendorf, H. U. Dodt, *Microsc. Res. Tech.* **2016**, *81*, 929–935.
[25] H. U. Dodt, U. Leischner, A. Schierloh, N. Jahrling, C. P. Mauch, K. Deininger, J. M. Deussing, M. Eder, W. Zieglgansberger, K. Becker, *Nat. Methods* **2007**, *4*, 331.
[26] M. K. Schwarz, A. Scherbarth, R. Sprengel, J. Engelhardt, P. Theer, G. Giese, *PLoS One* **2015**, *10*, e0124650.
[27] J. A. Riddick, W. B. Bunger, *Organic Solvents: Physical Properties and Methods of Purification*, New York, NY: Wiley-Interscience, **1970**.
[28] K. Valnes, P. Brandtzaeg, *J. Histochem. Cytochem.* **1985**, *33*, 755.
[29] K. I. Willig, R. R. Kellner, R. Medda, B. Hein, S. Jakobs, S. W. Hell, *Nat. Methods* **2006**, *3*, 721.
[30] U. Haupts, S. Maiti, P. Schwille, W. W. Webb, *Proc. Natl. Acad. Sci. U. S. A.* **1998**, *95*, 13573.
[31] R. F. Haseloff, I. E. Blasig, H. Meffert, B. Ebert Free Radic, *Biol. Med.* **1990**, *9*, 111.
[32] J. Llopis, J. M. McCaffery, A. Miyawaki, M. G. Farquhar, R. Y. Tsien, *Proc Natl Acad Sci U S A* **1998**, *95*, 6803.
[33] J. B. Treweek, V. Gradinaru, *Curr. Opin. Biotechnol.* **2016**, *40*, 193.
[34] F. Chen, P. W. Tillberg, E. S. Boyden, *Science* **2015**, *347*, 543.
[35] M. T. Ke, T. Imai, *Curr Protoc Neurosci* **2014**, *66*, 2.22.1.
[36] H. Hama, H. Hioki, K. Namiki, T. Hoshida, H. Kurokawa, F. Ishidate, T. Kaneko, T. Akagi, T. Saito, T. Saido, A. Miyawaki, *Nat. Neurosci.* **2015**, *18*, 1518.
[37] M. T. Ke, Y. Nakai, S. Fujimoto, R. Takayama, S. Yoshida, T. S. Kitajima, M. Sato, T. Imai, *Cell Rep.* **2016**, *14*, 2718.
[38] M. Halwer, *J. Am. Chem. Soc.* **1948**, *70*, 3985.
[39] Y. Qi, T. Yu, J. Xu, P. Wan, Y. Ma, J. Zhu, Y. Li, H. Gong, Q. Luo, D. Zhu, *Sci. Adv.* **2019**, *5*, eaau8355.

SUPPORTING INFORMATION

Additional supporting information may be found online in the Supporting Information section at the end of this article.

How to cite this article: Hahn C, Becker K, Saghafi S, et al. High-resolution imaging of fluorescent whole mouse brains using stabilised organic media (sDISCO). *J. Biophotonics*. 2019;12: e201800368. https://doi.org/10.1002/jbio.201800368